Cascade laser optimization for 3 H 4 → 3 H 5 and 3 F 4 → 3 H 6 sequent transitions in Tm 3+ -doped materials

Hippolyte Dupont, Lauren Guillemot, Pavel Loiko, Rosa Maria Solé, Xavier Mateos, Magdalena Aguiló, Francesc Díaz, Alain Braud, Patrice Camy, Patrick Georges, et al.

HAL Id: hal-04247277

https://hal-iogs.archives-ouvertes.fr/hal-04247277

Submitted on 18 Oct 2023

Cascade laser optimization for $^3H_4 \rightarrow {}^3H_5$ and $^3F_4 \rightarrow {}^3H_6$ sequent transitions in Tm^{3+}-doped materials

HIPPOLYTE DUPONT,[1,*] LAUREN GUILLEMOT,[2] PAVEL LOIKO,[2]
ROSA MARIA SOLÉ,[3] XAVIER MATEOS,[3] MAGDALENA AGUILÓ,[3]
FRANCESC DÍAZ,[3] ALAIN BRAUD,[2] PATRICE CAMY,[2]
PATRICK GEORGES,[1] AND FRÉDÉRIC DRUON[1]

[1] *Université Paris-Saclay, Institut d'Optique Graduate School, CNRS, Laboratoire Charles Fabry, 91127 Palaiseau, France*
[2] *Centre de Recherche sur les Ions, les Matériaux et la Photonique (CIMAP), UMR 6252 CEA-CNRS-ENSICAEN, Université de Caen, 6 Boulevard Maréchal Juin, 14050 Caen Cedex 4, France*
[3] *Física i Cristal·lografia de Materials (FiCMA), Universitat Rovira i Virgili (URV), 43007 Tarragona, Spain*
[*] *frederic.druon@institutoptique.fr*

Abstract: We study a cascade laser scheme involving the $^3H_4 \rightarrow {}^3H_5$ and $^3F_4 \rightarrow {}^3H_6$ consecutive transitions in Tm^{3+}-doped materials as a promising technique to favor laser emission at 2.3 µm. We examine the conditions in terms of the Tm^{3+} doping levels for which the cascade laser is beneficial or not. For this, Tm:LiYF$_4$ lasers based on crystals with several doping levels in the range of 2.5 - 6 at.% with and without cascade laser are studied. For low doping of 2.5 at.% Tm^{3+}, adding the laser emission at 1.9 µm allows to double the output power at 2.3 µm, whereas for high doping of 6 at.%, allowing the laser to operate at 1.9 µm totally suppresses the laser emission at 2.3 µm. An analytical model is developed and confronted with experimental results to predict this doping-dependent phenomenon and forecast the potential benefits. This study of cascade laser emission on the $^3H_4 \rightarrow {}^3H_5$ and $^3F_4 \rightarrow {}^3H_6$ transitions versus the Tm^{3+} doping level is finally extended to other well-known Tm^{3+}-doped laser materials.

1. Introduction

Laser sources emitting at 2.3 µm has seen a gain of interest in recent years due to the applications of such radiation for spectroscopy in the short-wave infrared spectral range. These sources are important, in particular, in the context of LIDAR systems, as their laser wavelengths are ideally located in the K-band of the atmosphere [1]. They are also useful for the study of combustion processes [2]. Various 2.3 µm sources have already been developed, notably based on optical parametric oscillators / amplifiers [3], semiconductor lasers [4] or solid-state lasers based on transition-metal or rare-earth ions directly emitting at this wavelength. Indeed, Cr^{2+}:ZnSe and Cr^{2+}:ZnS lasers cover the spectral range around 2.3 µm [5], as well as thulium (Tm^{3+}) based lasers operating on the $^3H_4 \rightarrow {}^3H_5$ electronic transition [6].

Tm-lasers have shown the advantage of being directly diode-pumped, whereas Cr^{2+}-based laser sources typically use Tm-lasers at 1.9 µm as pump sources. Direct laser emission at 2.3 µm from Tm^{3+}-doped materials has been a topic of multiple studies in the past few years. Tm-lasers emitting at 2.3 µm (on the $^3H_4 \rightarrow {}^3H_5$ transition) suffer from a strong competition with the high-gain $^3F_4 \rightarrow {}^3H_6$ transition, leading to emission around 1.9 µm. Various strategies have been developed to avoid colasing on this transition. The most common one consists of making unfavorable the undesired 1.9 µm laser using dichroic mirrors, i.e., those coated for high losses for the spectral range of the $^3F_4 \rightarrow {}^3H_6$ transition typically between 1.7 and 2.1 µm [7–9]. However, this strategy is not always the most successful one. In some cases, these losses are not sufficient

to avoid lasing at the $^3F_4 \rightarrow \, ^3H_6$ transition. This is notably the case of fiber lasers where Fresnel reflections on both the input and output facets of the fiber are sufficient for lasing around 1.9 µm [10–12]. The same problem can be observed for waveguide lasers whose gain is high [13]. Similarly, when using crystals with a strong electron-phonon interaction where phonon-assisted laser emission can be observed such as $Tm:Y_3Al_5O_{12}$ (shortly Tm:YAG) or $Tm:KLu(WO_4)_2$ (Tm:KLuW), the emission wavelength of lasers operating on the $^3F_4 \rightarrow \, ^3H_6$ laser transition can be strongly shifted towards 2.1 to 2.2 µm [14,15]. Since the wavelength of this emission is very close to that of the purely electronic $^3H_4 \rightarrow \, ^3H_5$ transition, it is technologically difficult to produce correct dichroic mirrors that introduce high losses in the range of 1.7 - 2.2 µm when low losses are required at 2.3 µm.

Due to these difficulties, an alternative strategy consists in taking the opposite of this technique by benefiting from the co-laser at 2.3 µm and 1.9 µm since they operate in cascade. This type of cascade laser has already been used in Tm^{3+},Ho^{3+}-codoped crystals to improve the efficiency of the 2.1 µm transition of holmium ions [16]. Publications using Tm^{3+}-doped $LiYF_4$ [17] and $CaGdAlO_4$ (CALGO) [18] also point out the potential advantage of this strategy. They show in different configurations how the addition of the 1.9 µm transition allows a significant increase in the laser emission at 2.3 µm. The improvement in laser efficiency is mainly explained by recycling of thulium ions stored in the metastable intermediate $^3F_4$ level, which are forced down to the ground-state level. These two cascade lasers thus avoid the bottleneck effect in the metastable median electronic level being typical for 2.3 µm thulium lasers. On the other hand, the population reduction of the $^3F_4$ level by adding a laser transition at 1.9 µm also strongly reduces the energy transfer upconversion (ETU) from this level. The latter process contributes to improvement of the laser efficiency at 2.3 µm since it helps to populate the upper laser level [19]. Consequently, ETU between two thulium ions in the $^3F_4$ state allows to send one ion to the $^3H_4$ level and one - to the $^3H_6$ ground-state, and it modifies the 2.3 µm laser population rate as well as the absorption saturation process when Tm^{3+} ions are pumped at 790 nm. Since both the absorption and the ETU are strongly concentration-dependent [19], we expect that the effect of a laser cascade will not be always beneficial and will be doping level dependent.

In the present paper, we investigate this doping question for the first time to our best knowledge. First, the effect of cascade laser for different Tm^{3+} doping levels is studied experimentally for the well-known and largely-used $Tm:LiYF_4$ crystal. Several questions are addressed. Over which range of doping concentration is the cascade laser beneficial for 2.3 µm laser emission and for which is it detrimental and must be avoided? Is there an accessible optimal doping level? And what improvement in terms of laser efficiency can be expected? To answer these questions, we parallelly developed a simple analytical predictive model and confronted it to the experimental data obtained with Tm: $LiYF_4$. To conclude our study, we also extend the use of our model to evaluate the potential cascade laser benefice for other Tm^{3+}-doped crystals.

2. Experimental setup

To study cascade laser emission from a Tm-laser, we construct a partially overlapped dual laser cavity allowing for simultaneous laser operation at 1.9 µm and 2.3 µm. The Tm^{3+}-doped laser crystal is pumped by a continuous-wave Ti:Sapphire laser emitting up to 2.5 W around 780 nm. A focusing lens with an optimized focal length of 100 mm is used to focus the pump radiation into the crystal. The pump beam waist diameter is 43 µm in the crystal. To separate the emission on the $^3H_4 \rightarrow \, ^3H_5$ transition and that on the $^3F_4 \rightarrow \, ^3H_6$ one, we build two nested V-cavities of identical size so that the two waists of the cavities perfectly overlap in the crystal. They share the pump mirror, the laser crystal and a plano-concave mirror with a radius of curvature (RoC) of −200 mm. The two cavities are separated using a dichroic mirror coated for high reflection (HR, R > 99.95% at 2.15 −2.4 µm) and high transmission (HT, T > 99.5% at 1.7-2.1 µm). An additional mirror with the same features is used as a filter to avoid any 2.3 µm laser transition in

the "1.9 μm – laser" arm. The two cavities are closed by two independent output couplers (OCs). The pump mirror is coated for HR at 2.2-2.4 μm and has a transmission of 5% at 1.9 μm. The distance between the pump mirror and the concave plane mirror is experimentally optimized around 105 mm. The distance between the latter mirror and the two output couplers is 350 mm for both cavities. For the cavity arm supporting the $^3F_4 \rightarrow {}^3H_6$ laser transition, the OC provides a transmission of 2% at 1.70 - 1.95 μm, and for the second cavity arm supporting the $^3F_4 \rightarrow {}^3H_6$ transition, the output coupling is 3% at 2.1 - 2.4 μm.

3. Tm:LiYF$_4$ cascade laser

3.1. Laser crystals

We select the Tm:LiYF$_4$ crystal for experimental demonstration of the cascade Tm-laser as this crystal is currently one of the most commonly used materials for lasers at 2.3 μm due to its good spectroscopic and thermal properties, as well as commercial availability.

Let us briefly describe the spectroscopic properties of Tm^{3+} ions in this material. For the $^3H_6 \rightarrow {}^3H_4$ pump transition, the maximum absorption cross-section σ_{GSA} is 0.64×10^{-20} cm^2 at 781 nm for π-polarization [20]. For the considered laser transitions, the stimulated-emission cross-sections σ_{SE} are 0.42×10^{-20} cm^2 at 1877 nm (the $^3F_4 \rightarrow {}^3H_6$ transition) [21] and 0.52×10^{-20} cm^2 at 2303 nm (the $^3H_4 \rightarrow {}^3H_5$ transition) for π-polarized light [22]. The ion density corresponding to a Tm^{3+} doping level of 1 at.% is 1.38×10^{20} cm^{-3}. The intrinsic lifetimes of the $^3F_4$ and $^3H_4$ levels (for low Tm^{3+} doping levels) are 11 ms and 2.3 ms, respectively.

For our study, three Tm:LiYF$_4$ crystals with different doping levels are used and their parameters are listed in Table 1. The crystal thicknesses are chosen to provide pump absorption at 781 nm around 80%. All crystals are antireflection coated for both the pump and laser wavelengths to avoid Fresnel losses.

3.2. Experimental result

The Tm:LiYF$_4$ crystal is positioned in the double cavity described in Fig. 1(b). To observe the influence of the 1.9 μm laser emission on the 2.3 μm one, the input-output dependences (i.e., the output power at 2.3 μm vs. the pump power at 780 nm) are measured for all the studied laser crystals. The 1.9 μm laser emission is allowed or not by using a pinhole depending on whether the cascade laser is desired or not without changing any alignments.

The experimental results presented in Fig. 2 show different cases in which the presence of the cascade laser involving the emission at 1.9 μm is favorable or unfavorable for the laser at 2.3 μm, as a function of different doping level. For the highest studied concentration of Tm^{3+} ions of 6 at.%, by allowing the laser to operate on the $^3F_4 \rightarrow {}^3H_6$ transition, no laser emission at 2.3 μm is observed. Without the cascade laser scheme, the output power amounts to 90 mW at 2.3 μm but it drops to zero when the 1.9 μm laser operates. As a result, the cascade laser scheme is clearly in disfavor of the 2.3 μm emission. In contrast, for a doping level of 2.5 at.%, the addition of the laser cascade at 1.9 μm increases the output power at 2.3 μm from 90 mW to 180 mW, i.e., representing a two-fold increase. For an intermediate Tm^{3+} concentration of 3 at.%, by allowing the laser to operate at 1.9 μm, the increase of the output power at 2.3 μm is less significant, namely from 200 mW to 248 mW (24% variation).

To understand the involved phenomena, the pump absorption efficiency at 781 nm is measured in three different regimes, namely, first, when the laser operates on the cascade scheme, second, when only the laser emission at 2.3 μm is supported and third, without any laser operation. Compared to the case of purely 2.3 μm laser emission, by allowing the laser to operate on the $^3F_4 \rightarrow {}^3H_6$ transition, the pump absorption increases by 45%, 22% and 19% for 2.5 at.%, 3 at.%, and 6 at.% Tm^{3+} doping, respectively. The 2.3 μm laser emission also leads to an increase of the pump absorption compared to the case without any laser action but in a less extent. The

Table 1. Parameters Used in the Simulation of the Cascade Laser Performance

| Notation	Parameter	Value		
η_{780nm}	Quantum defect	33.9%		
σ_a	Absorption cross section at 780 nm	0.64×10^{-20} cm^2		
P_p	Input power for the pump at 780 nm	0 - 2.5 W		
V	Volume of the useful gain medium: determined using the waist ω	2.4×10^{-10} m^{-3} ω = 20 µm (FWHM) M^2=1.1		
$P_{2.3\mu m}$	Output power at 2.3 µm	Output of the code (W)		
$N_{^3H_4}$	Population of the ^{3}H$_4$ level in CW laser regime imposed by the cavity losses (4%)	9×10^{18} cm^{-3}		
	Depending of the crystal	No.°1	No.°2	No.°3
N	Concentration of thulium ions (10^{20} cm^{-3})	3.4	4.1	8.6
	Doping (at.%)	2.5	3	6
l	Length of the crystal (mm)	8	8	5
$n_{^3F_4\ c}$	Normalized population of the ^{3}F$_4$ level in cascade laser operation	40%	58%	63%
$n_{^3F_4\ nc}$	Normalized population of the ^{3}F$_4$ level without cascade laser	85%	78%	67%
$N_{^3F_4\ x}$	Population of the ^{3}F$_4$ level with $x \in \{c, nc\}$		$N\ n_{^3F_4\ x}$	
A_{nc}	Pump absorption without cascade laser operation	30%	52%	60%
A_c	Pump absorption in cascade laser operation	75%	70%	79%
K_{ETU}	ETU parameter (10^{-20} cm^{3}s^{-1}), cf. Figure 5(e)	2.4	6.6	38
η_c	Slope efficiency of the 2.3 µm laser vs. absorbed pump power in the case of cascade laser	18%	15%	-
η_{nc}	Slope efficiency of the 2.3 µm laser vs. absorbed pump in absence of cascade laser	19%	18%	20%
η_{opt}	Efficiency of extraction of 2.3 µm laser radiation with the relation $\eta_c = \eta_{opt}\eta_{780nm}$	54%	51%	-
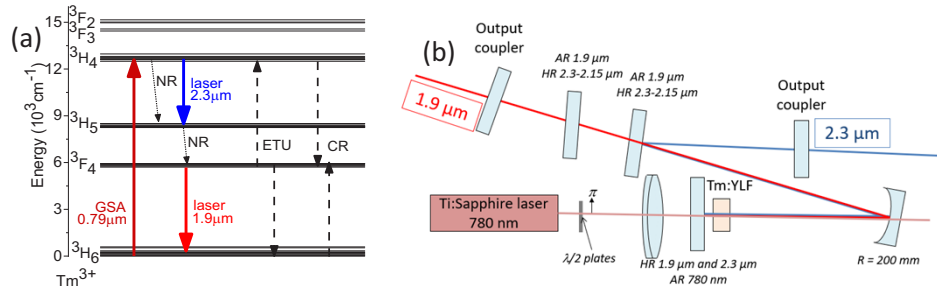
Fig. 1. (a) Energy-level scheme for Tm^{3+} ions in LiYF$_4$ showing processes relevant for the cascade laser study: GSA – ground-state absorption, CR – cross-relaxation, ETU – energy-transfer up-converion, NR – multiphonon non-radiative relaxation; (b) Scheme of the laser set-up used for the cascade laser study in Tm:LiYF$_4$.

observed increase in the pump absorption under cascade laser operation is the principal reason to explain the increase in the output power at 2.3 µm simply due to the increased pumping efficiency. However, this explanation is not sufficient since similar increases in absorption are measured for 3 at.% and 6 at.% Tm^{3+} doping levels but the effects on the 2.3 µm laser emission are radically
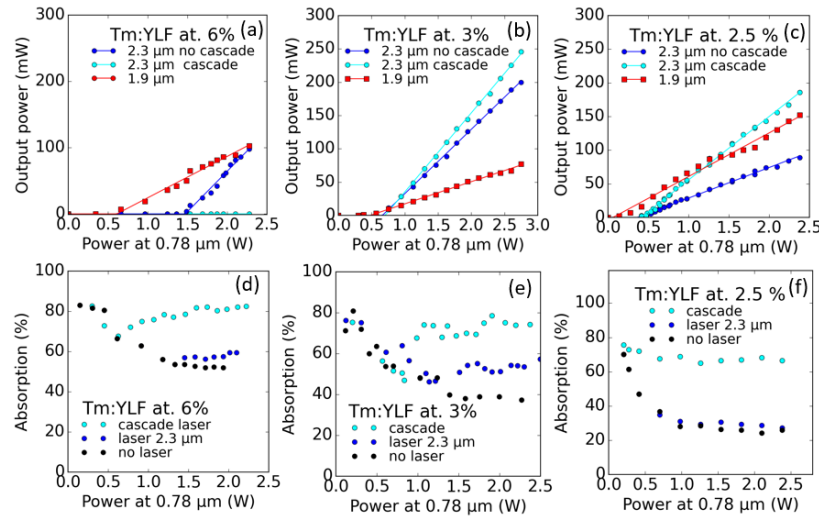
Fig. 2. Cascade Tm:LiYF$_4$ lasers: (a-c) Output power at 2.3 µm and 1.9 µm and (d-f) pump absorption efficiency at 781 nm. The Tm^{3+} doping level is (a,d) 6 at.%, (b,e) 3 at.%, and (c,f) 2.5 at.%.

different. The differences in the impact of the 1.9 µm laser channel on the 2.3 µm one can nevertheless be explained by the fact that adding the emission at 1.9 µm empties the ^{3}F$_4$ level population. Emptying this manifold also reduces the influence of the ETU which helps to fill the upper laser level for the ^{3}H$_4 \rightarrow$ ^{3}H$_5$ transition.

3.3. Modeling of laser performance

To further understand the effect of Tm^{3+} doping concentration on the laser performance and the other physical quantities involved, an analytical model is proposed. The aim is to analyze the variation of the laser power at 2.3 µm due to variations in the pump absorption and ETU rates. The notations and values used in the present work are summarized in Table 1.

In this model, the variation of the laser output at 2.3 µm is assumed to be due to two main reasons: first, the variation of the pump absorption efficiency and second, the variation of the ETU efficiency refilling the upper laser level (^{3}H$_4$): $\Delta P_{2.3\mu m} = \Delta P_{2.3\mu m,abs} + \Delta P_{2.3\mu m,ETU}$. The increase in the output power due to increased pump absorption is quantified as follows: $\Delta P_{2.3\mu m,abs} = P_p(\eta_c A_c - \eta_{nc} A_{nc})$. Assuming that the cascade laser operation mainly induces mainly a variation of pump absorption with low perturbation of the laser slope efficiency, η_c and η_{nc} can be considered to be equal: $\Delta P_{2.3\mu m,abs} = P_p \eta_c \Delta A$. This simplifying assumption (which is valuable from the predictive point of view) is of course not valid when the cascade laser scheme prevents oscillations at 2.3 µm laser so that $\eta_c = 0$ and the model is clearly less precise in such a case (which corresponds to the case of 6 at.% Tm:LiYF$_4$ laser for example). The change in absorption $\Delta A = A_c - A_{nc}$ can either be directly determined from the previously described absorption measurements or simply calculated from the Beer-Lambert law. For such a calculation, a simplification assumption is made that all the Tm^{3+} ions are either in the fundamental ^{3}H$_6$ level, or they are accumulated in the metastable ^{3}F$_4$ level. Considering the long lifetime of this level compared to the fluorescence lifetime of the ^{3}H$_4$ manifold quenched by the cross-relaxation process [23–24], this assumption is in general valid. In our case, since the laser at 2.3 µm empties furthermore the ^{3}H$_4$ level, it become acceptable. In addition, the ^{3}H$_5$ level is rapidly thermally relaxed to the lower-lying ^{3}F$_4$ level and its population is nearly negligible, so that the absorption

can be calculated as $A_x = 1 - e^{-\sigma_a lN(1-n_{^3F_4\,x})}$ with $x \in \{c, nc\}$ (with c for "cascade" and nc for "no cascade").

For the power variation at 2.3 μm due to the ETU, a quantification can be defined as follows, based on the rate equations [23]:

$$\left[\frac{dN_{^3H_4}}{dt}\right]_{ETU,\,x} = K_{ETU}N_{^3F_4\,x}^2 = K_{ETU}N^2 n_{^3F_4\,x}^2. \tag{1}$$

If we assume that the ions that arrive to the $^3H_4$ level contribute to emission at 2.3 μm with the probability η_{opt}, the power variation can be evaluated with the following equation:

$$\Delta P_{2.3\,\mu m,\ ETU} = \eta_{opt}h\upsilon\,VK_{ETU}N^2(\,n_{^3F_4\,c}^2 - n_{^3F_4\,nc}^2\,). \tag{2}$$

To determine the active volume (V) in the crystal, we consider the divergence of the beam by calculating the volume inside the intersection between the pump hyperboloid and the crystal. The K_{ETU} parameter is a key value as it strongly depends on the doping level. Since it is not easily accessible, it is often considered that it changes linearly with the ion density. The parameters given in the literature [19,25–27] for the Tm:LiYF$_4$ crystal and those used in the present paper are plotted in Fig. 3. An interpolation can also be plotted using literature data, it can be likewise used as an alternative to the linear fit to estimate K_{ETU} in our model.
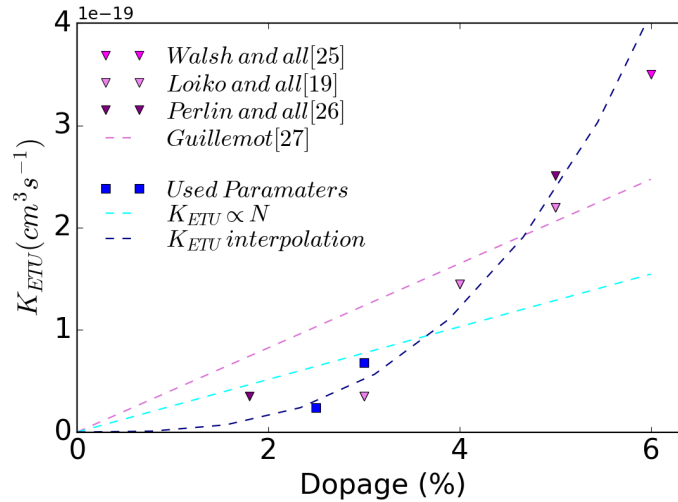

Fig. 3. The energy-transfer upconversion parameter K_{ETU} vs. Tm^{3+} doping level in LiYF$_4$. *Triangles* – literature data [19,25–27], *squares* – the K_{ETU} values used in the present work.

Note that the power variation in this equation intrinsically depends on the cavity architecture through the parameters η_c and η_{opt}. To limit the number of free parameters in the model, we therefore focus our interest on the normalized power variation, i.e., by dividing the power variation by the output power in the presence of the cascade laser operation:

$$\frac{\Delta P_{2.3\,\mu m}}{P_{2.3\,\mu m\,c}} = \frac{\Delta P_{2.3\,\mu m}}{\eta_c P_p A_c} = \frac{\Delta A}{A_c} + \frac{h\nu}{P_p A_c \eta_{780nm}}\,V\,K_{ETU}N^2\Delta(n_{^3F_4}^2). \tag{3}$$

The power variation at 2.3 μm divided by the power at 2.3 μm without cascade laser can be obtained by changing the variable: $\frac{\Delta P_{2.3\,\mu m}}{P_{2.3\,\mu m\,nc}} = \frac{\Delta P_{2.3\,\mu m}/P_{2.3\,\mu m\,c}}{1-\Delta P_{2.3\,\mu m}/P_{2.3\,\mu m\,c}}$. Note that the value $\frac{\Delta P_{2.3\,\mu m}}{P_{2.3\,\mu m\,c}}$ can

tend towards large negative values without being bounded. Because of this, the choice of dividing by $P_{2.3\,\mu m\,nc}$ appears more pertinent since intrinsically, it has a lower bound limited at -100%.

The present model is then compared with the experimental measurements made with the Tm:LiYF$_4$ crystals to qualify it and verify that it could be useful to fairly predict the variations in laser efficiencies of cascade Tm-lasers based on crystals with different doping levels. The $n^2_{^3F_4\,x}$ values are estimated using the absorption curves. Since the different tested crystals have different pump absorption efficiencies and / or thicknesses, this would imply a model with different input parameters for each one. It is particularly the $n^2_{^3F_4\,x}$ parameter that is dependent on the doping level because the energy-transfer upconversion tends to empty the $^3F_4$ level for high doping levels (see Table 1).

Since the goal of the present study is to provide an estimation of the tendency from the point of view of having a semi-empirical predictive model, we are plotting this curve using only one variable parameter, i.e., the doping concentration. Because of this, we decide to take the average values for the other parameter, acknowledging that these ones could varying in a limited extend, especially $n^2_{^3F_4\,x}$. We then use the set of values of 83%, 50%, 8 mm for the parameters $n^2_{^3F_4\,nc}$, $n^2_{^3F_4\,c}$ and l, respectively, to obtain a unique trend curve that could have been predicted. The K_{ETU} value is obtained using both a linear model (with a concentration-independent coefficient of 0.8×10^{-40} cm^{6}s^{-1}) or the interpolation based on the literature data, as shown in Fig. 3. Considering these values and the different hypotheses, the model gives good evidence of cases when the cascade laser emission is beneficial but remains overestimating for high doping levels. Indeed, the K_{ETU} parameter increases significantly for constant $n^2_{^3F_4\,x}$ whereas this population may decrease and compensate the increase of K_{ETU}. Anyway, the model allows to have a good estimate especially for the interesting points at low doping levels and a physically coherent tendency for higher doping. Furthermore, changing of the $n^2_{^3F_4\,x}$ parameter has a very low influence on the crossroads of the normalized power variation $\frac{\Delta P_{2.3\,\mu m}}{P_{2.3\,\mu m\,c}}$ with the zero axis, that is the keystone to know whether a cascade laser scheme is beneficial or not.
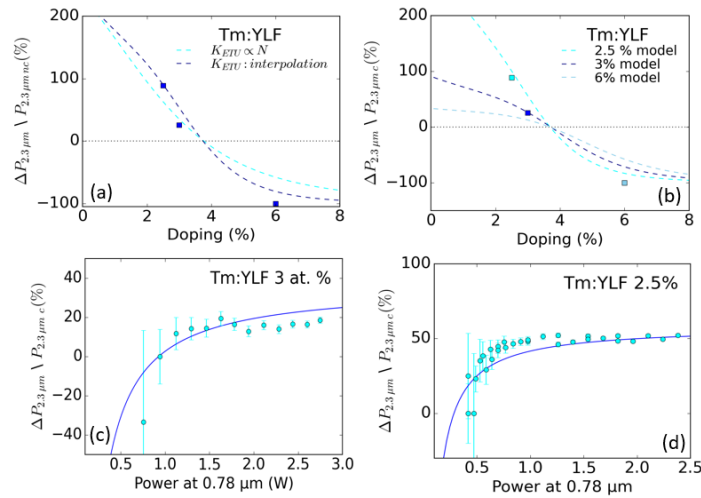

Fig. 4. Normalized power variation for laser emission at 2.3 µm from cascade Tm:LiYF$_4$ lasers: (a,b) effect of the doping concentration, *symbols* – experimental data, *curves* - theoretical modeling: calculations using (a) averaged or (b) exact experimental data for each crystal; (c,d) effect of the pump power at 781 nm: *symbols* – experimental data, *curves* - theoretical modeling for (c) 3 at.% Tm:LiYF$_4$ and (d) 2.5 at.%. Tm:LiYF$_4$.

Despite a simple model based on several assumptions described above, we obtained a semi-empirical equation accurately reproducing the trend observed experimentally. To answer the question whether the model could be more precise considering the data measured for each particular crystal and not the average values, we plot in Fig. 4 the simulation results for the 2.5 at.% and 3 at.% Tm^{3+}-doped $LiYF_4$ crystals. As expected, the agreement becomes more precise. Moreover, one can observe that the limit where the cascade laser is advantageous does not vary for the different curves. To be able to test this model with more experimental points, we also plot for the two above-mentioned crystals the same normalized power variations with the cascade laser for various pump powers as shown in Fig. 4(c,d). For these curves, the variables $n^2_{^3F_4\,nc}$, $n^2_{^3F_4\,c}$ and K_{ETU} are the ones corresponding to each crystal. The values of K_{ETU} for both crystals have been added to Fig. 3.

It can be seen that for the 3 at.% Tm^{3+}-doped crystal, the value $\Delta P_{2.3\,\mu m}/P_{2.3\,\mu m\,c}$ reaches 19.5% while the relative absorption difference $\Delta A/A_c$ approaches 25%. This result corresponds well to those expected by our model, as $\Delta P_{2.3\,\mu m}/P_{2.3\,\mu m\,c}$ tends towards the relative absorption difference when the pump power becomes sufficiently high. For the 2.5 at.% Tm^{3+}-doped crystal, the measured value of $\Delta P_{2.3\,\mu m}/P_{2.3\,\mu m\,c}$ reaches 49.2% while the relative variation in absorption is 53%. One may observe that, for the pump powers closer to the threshold, the model becomes less accurate. It can be explained by the fact that the assumption $\eta_c \sim \eta_{nc}$ is no longer valid in this case.

4. Extension of the analytical model to diode-pumping

Using fiber-coupled laser diodes for pumping Tm^{3+}-doped crystals instead of Ti:Sapphire lasers allows for design of power-scalable and compact systems. The main difference consists of the available power and beam quality (brightness) of pumps. As a consequence, it is interesting to adapt our model and to trace the impact of this change on the predicted cascade laser effect since it is mainly affects the term related to the ETU process through the available pump power and the pump volume such as:

$$\left[\frac{\Delta P_{2.3\,\mu m}}{P_{2.3\,\mu m\,c}}\right]_{ETU} \propto \frac{V}{P_p} \sim \frac{l}{I_p}. \tag{4}$$

Commercial fiber-coupled laser diodes offer high-power output at the expense of lower spatial beam quality (lower brightness). Therefore, the change of the pump source could affect the cascade laser effect. We notice that at a constant pump intensity, the effect remains globally the same. Indeed, at a constant intensity, the pump absorption and the population of the $^3F_4$ level will also remain unchanged. Current powerful laser diodes allow one to access to this order of magnitude of laser intensity as demonstrated in the literature for diode-pumped Tm:$LiYF_4$ lasers at 2.3 µm and 1.9 µm by *Huang* et al. [17]. In this work, the power at 2.3 µm amounted to 650 mW (with cascade laser emission) and only 350 mW (without cascade laser). This experimental point is added to Fig. 5(a) to provide a comparison with our model. It is important to note that this new independent experimental point validates the presented model for diode pumping for yet lower Tm^{3+} doping level than those studied in the present work.

In Fig. 5, simulations for this diode emitting up to 25 W of output power focused into a spot of 200 µm [17] is also presented. For comparison, we plot simulated curves for two previously reported diode-pumping schemes with Tm:YLF crystal : 90 W output, focused into a waist of 260 µm [28] and 450 W output, 500 µm spot ($M^2 \sim 150$) [29] as shown in Fig. 5(a). The conclusion is that the optimization of cascade implies slightly lower doping levels for the diode pumping but remains relatively equivalent, and the model can be extended easily to the diode-pumped configurations.
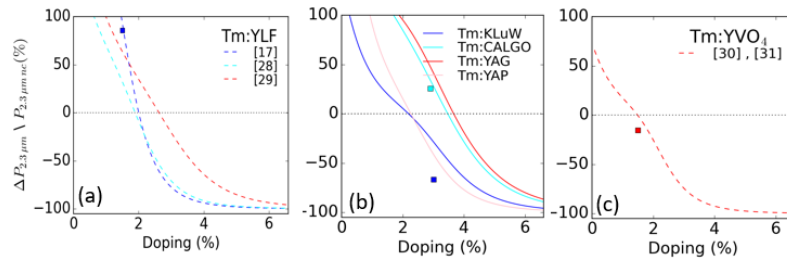
Fig. 5. Normalized power variation for laser emission at 2.3 μm from cascade diode-pumped Tm-lasers: (a) For diode-pumped Tm:LiYF$_4$ lasers already described in the literature, theoretical modeling of $\Delta P_{2.3\,\mu m}/P_{2.3\,\mu m\,c}$ vs. the doping level corresponds to parameters described in the text and the experimental point is coming from Huang et al. [17]; (b) For several Ti:Sapphir pumped Tm^{3+}-doped crystals, experimental (*symbols*) and theoretical modeling (*curves*) data are also shown. (c) For diode-pumped Tm:YVO$_4$, theoretical modeling of $\Delta P_{2.3\,\mu m}/P_{2.3\,\mu m\,c}$ vs. the doping level corresponds to parameters described in the text. The experimental point is coming from *Yu et al.* [30,31];

5. Confrontation of the analytical model with other crystals

Other crystals than Tm:LiYF$_4$ also demonstrated cascade laser emission at 2.3 μm and 1.9 μm, such as Tm:CALGO [18] and appeared promising for emission at 2.3 μm for different reasons (e.g., broadband emission properties). It is interesting to see if our model can be extended to other Tm^{3+}-doped materials. From the previous results for Tm:CALGO, the relative variation of the power at 2.3 μm vs. the doping level can be plotted to compare the experimental and simulated results. An output power at 2.3 μm of 332 mW (with cascade laser emission) and only 264 mW (without cascade laser) was reported for an incident pump power of 2.5 W. Concerning the modelling for Tm:CALGO, the population of the ^{3}F$_4$ level is fixed at 55% with cascade laser against 90% without it, according to the measured pump absorption efficiency (75% with cascade laser and 63% without it) given in [18].

Yu et al., demonstrated diode pumped cascade lasing in Tm:YVO$_4$ [30,31] and Tm:GdVO$_4$ with an output power of 2.88 W at 2.3 μm [32]. Refence [30,31] presented by the authors show a 1.5 at. % Tm:YVO$_4$ crystal in the same configuration changing only the coating of the output coupler to have or no cascade laser at 1.9 μm. With an incident pump power of 25 W and an output coupler of 1% at 2.3 μm, the output power is 1.1 W with cascade laser [30] and 1.3 W without cascade laser [31]. The calculation showed a lower efficient cascade laser in these crystals : indeed the absorption is still high under no lasing condition, so that the gain that consist of increasing the absorption is low. For the model, the population of the ^{3}F$_4$ level is estimated to be 45% with the cascade laser and 70% without it.

To provide another comparison, we also look at the Tm:KLuW crystal which is particular since the long-wave phonon sideband of the ^{3}F$_4 \rightarrow\ ^3$H$_6$ electronic transition extends up to at least 2.2 μm. To our best knowledge, the influence of the cascade laser scheme on the 2.3 μm laser emission of this crystal has not been reported so far. The crystal used in the present study is 3.0 at.% Tm^{3+}-doped and 5 mm long. For the laser cavity, a CaF$_2$ prism is added into the arm supporting laser oscillations at 2.3 μm to avoid any vibronic cascade laser emission in the spectral range of 2.1-2.2 μm. The pump polarization is chosen to be $\boldsymbol{E}$ || N_{p} in the crystal corresponding to an absorption cross-section of $\sigma_{\mathrm{GSA}} = 9.96 \times 10^{-20}$ cm^2 at 793 nm. The power obtained at 2.29 μm is 10 mW (in the presence of cascade laser emission), compare with 30 mW without cascade laser at 1.9 μm, making the cascade laser scheme unfavorable in this case. It can be explained by a small difference of pump absorption between the two configurations (95% without the cascade laser effect, 99% with it), making the improvement in the absorption efficiency marginal. For the

model, the population of the $^3F_4$ level is estimated to be 40% with the cascade laser and 75% without it. The difference between measurement and calculation can be explained by the fact that the laser operates close to the laser threshold. The assumption $\eta_c \sim \eta_{nc}$ is no longer valid in this case.

We decided to compare these experimental results with three different crystals with our analytical model. However, as the coefficient K_{ETU} (as well as its concentration dependence) is not well referenced for other crystals as it is done for Tm:LiYF$_4$, we have to find a solution to evaluate these parameters for our model. The cross-relaxation coefficients are usually better referenced in literature. Considering that ETU and cross-relaxation are related effects (they are antagonistic effects), we assume that the ratio between their coefficients can be considered equivalent for Tm:LiYF$_4$ and other crystals used in our model. It is then possible to compare the experiment and the analytical model, as shown in Fig. 5(b). It is interesting to note that even with some lacune for certain spectroscopic data for the considered crystals, the numerical simulations are in relatively good agreement with the experimental results, indicating a low dispersion of the missing parameters between crystals and validating the extension of the model to other Tm^{3+}-doped materials. It can be explained by the fact that the optimal laser crystals are often designed to have similar pump absorption, lengths within a typical range of doping levels. Being confident in our model, we also plot in Fig. 5(b) the prediction for Tm:YAG and Tm:YAP which is also a crystal of interest.

6. Conclusion

In conclusion, we studied positive effect of the cascade laser involving the $^3H_4 \rightarrow ^3H_5$ and $^3F_4 \rightarrow ^3H_6$ consecutive laser transitions in Tm:LiYF$_4$ and answered the question how the addition of laser emission at 1.9 μm can improve the output at 2.3 μm. This improvement strongly depends on the thulium doping concentration, and it can mainly be explained by a significant increase in the pump absorption, counterbalanced by the negative effect of ETU. An analytical model to evaluate this phenomenon is developed. Corroborated with experimental studies on three LiYF$_4$ crystals doped with 2.5 - 6 at. %, this model shows that, in some configurations, the addition of a laser cascade can double the output at 2.3 μm. The cascade laser technique is shown to be an alternative way of pump recycling to improve the efficiency of thulium-based 2.3 μm lasers. It has the advantage of being implemented simply by ensuring that the used laser mirrors provide high reflectivity additionally around 1.9 μm, given that they must already be reflective at 2.3 μm. These mirrors are often easier and less constrained to produce than dichroic mirrors that are currently used. Moreover, in the case of Tm:YAG and Tm:KLuW crystals where emission on the $^3F_4 \rightarrow ^3H_6$ transition is possible between 2.0 and 2.2 μm using the phonon assisted mechanism, using the cascade laser is even more critical. After validation, the simple presented analytical model was extended, using several fair hypotheses, to be a predictive model for different practical configurations such as diode pumping and other Tm^{3+}-doped materials. The numerical results have been confronted with various host matrices based on the results available in the literature, and they are in line with the experiments. Thus, the model allows one to estimate the range of Tm^{3+} doping levels for which cascade laser is advantageous for boosting the laser efficiency at 2.3 μm.

Disclosures. The authors declare no conflicts of interest.

Data availability. Data underlying the results presented in this paper are not publicly available at this time but may be obtained from the authors upon reasonable request.

References

1. G. G. Taylor, D. Morozov, N. R. Gemmell, K. Erotokritou, S. Miki, H. Terai, and R. H. Hadfield, "Photon counting LIDAR at 2.3 μm wavelength with superconducting nanowires," Opt. Express **27**(26), 38147–38158 (2019).

2. F. J. McAleavey, J. O'Gorman, J. F. Donegan, B. D. MacCraith, J. Hegarty, and G. Maze, "Narrow linewidth, tunable Tm^{3+}-doped fluoride fiber laser for optical-based hydrocarbon gas sensing," IEEE J. Sel. Top. Quantum Electron. **3**(4), 1103–1111 (1997).

3. V. Petrov, "Frequency down-conversion of solid-state laser sources to the mid-infrared spectral range using non-oxide nonlinear crystals," Prog. Quantum Electron. **42**, 1–106 (2015).

4. A. Salhi, Y. Rouillard, A. Pérona, P. Grech, M. Garcia, and C. Sirtori, "Low-threshold GaInAsSb/AlGaAsSb quantum well laser diodes emitting near 2.3 µm," Semicond. Sci. Technol. **19**(2), 260–262 (2004).

5. I. Moskalev, S. Mirov, M. Mirov, S. Vasilyev, V. Smolski, A. Zakrevskiy, and V. Gapontsev, "Ultrafast middle-IR lasers and amplifiers based on polycrystalline Cr:ZnS and Cr:ZnSe," Opt. Mater. Express **7**(7), 2636–2650 (2017).

6. J. Caird, L. DeShazer, and J. Nella, "Characteristics of room-temperature 2.3-µm laser emission from Tm3 + in YAG and YAlO₃," IEEE J. Quantum Electron. **11**(11), 874–881 (1975).

7. E. Kifle, P. Loiko, L. Guillemot, J.-L. Doualan, F. Starecki, A. Braud, T. Georges, J. Rouvillain, and P. Camy, "Watt-level diode-pumped thulium lasers around 2.3 µm," Appl. Opt. **59**(25), 7530–7539 (2020).

8. L. Guillemot, P. Loiko, R. Soulard, A. Braud, J.-L. Doualan, A. Hideur, and P. Camy, "Close look on cubic Tm:KY₃F₁₀ crystal for highly efficient lasing on the $^3H_4 \to {}^3H_5$ transition," Opt. Express **28**(3), 3451–3463 (2020).

9. L. Guillemot, P. Loiko, A. Braud, J.-L. Doualan, A. Hideur, M. Koselja, R. Moncorge, and P. Camy, "Continuous-wave Tm:YAlO₃ laser at ~2.3 µm," Opt. Lett. **44**(20), 5077–5080 (2019).

10. B. I. Denker, V. V. Dorofeev, B. I. Galagan, V. V. Koltashev, S. E. Motorin, V. G. Plotnichenko, and S. E. Sverchkov, "A 200 mW, 2.3 µm Tm^{3+}-doped tellurite glass fiber laser," Laser Phys. Lett. **17**(9), 095101 (2020).

11. J. N. Carter, D. C. Hanna, R. G. Smart, and A. C. Tropper, "Thulium-doped fluorozirconate fiber lasers operating at around 0.8, 1.47, 1.9, and 2.3 µm pumped at 0.79 µm," in *Advanced Solid State Lasers* (OSA, 1991), p. MIL13.

12. C. Jia, B. J. Shastri, P. R. Prucnal, M. Saad, and L. R. Chen, "Simultaneous Q-switching of a Tm^{3+}:ZBLAN fiber laser at 1.9 µm and 2.3 µm using graphene," IEEE Photonics Technol. Lett. **29**(4), 405–408 (2017).

13. R. Soulard, P. Loiko, G. Brasse, J.-L. Doualan, A. Braud, A. Tyazhev, A. Hideur, B. Guichardaz, L. Guillemot, F. Druon, and P. Camy, "Efficient bulk and waveguide Tm:LiYF4 lasers at 2306 nm," in *Laser Congress 2018 (ASSL)* (OSA, 2018), p. ATu2A.32.

14. L. Guillemot, P. Loiko, E. Kifle, J.-L. Doualan, A. Braud, F. Starecki, T. Georges, J. Rouvillain, A. Hideur, and P. Camy, "Watt-level mid-infrared continuous-wave Tm:YAG laser operating on the $^3H_4 \to {}^3H_5$ transition," Opt. Mater. **101**, 109745 (2020).

15. P. Loiko, E. Kifle, L. Guillemot, J.-L. Doualan, F. Starecki, A. Braud, M. Aguiló, F. Díaz, V. Petrov, X. Mateos, and P. Camy, "Highly efficient 2.3 µm thulium lasers based on a high-phonon-energy crystal: evidence of vibronic-assisted emissions," J. Opt. Soc. Am. B **38**(2), 482 (2021).

16. R. C. Stoneman and L. Esterowitz, "Continuous-wave 1.50-µm thulium cascade laser," Opt. Lett. **16**(4), 232–234 (1991).

17. H. Huang, S. Wang, H. Chen, O. L. Antipov, S. S. Balabanov, and D. Shen, "High power simultaneous dual-wavelength CW and passively-Q-switched laser operation of LD pumped Tm:YLF at 19 and 23 µm," Opt. Express **27**(26), 38593 (2019).

18. Hippolyte Dupont, Pavel Loiko, Aleksey Tyazhev, Luidgi Giordano, Zhongben Pan, Hongwei Chu, Dechun Li, Bruno Viana, Ammar Hideur, Lauren Guillemot, Alain Braud, Patrice Camy, Patrick Georges, and Frédéric Druon, "Tm:CALGO lasers at 2.32 µm: cascade lasing and upconversion pumping," Opt. Express **31**(12), 18751–18764 (2023).

19. P. Loiko, P. Camy, R. Soulard, L. Guillemot, G. Brasse, J.-L. Doualan, A. Braud, A. Tyazhev, A. Hideur, and F. Druon, "Efficient Tm:LiYF₄ lasers at 2.3 µm: Effect of energy-transfer upconversion," IEEE J. Quantum Electron. **55**(6), 1–12 (2019).

20. I. Razumova, A. Tkachuk, A. Nikitichev, and D. Mironov, "Spectral-luminescent properties of Tm:YLF crystal," J. Alloys Compd. **225**(1-2), 129–132 (1995).

21. U. Demirbas, J. Thesinga, M. Kellert, F. X. Kärtner, and M. Pergament, "Temperature dependence of the fluorescence lifetime and emission cross section of Tm:YLF in the 78–300 K range," Opt. Mater. Express **12**(12), 4712–4732 (2022).

22. P. Loiko, J.-L. Doualan, L. Guillemot, R. Moncorgé, F. Starecki, A. Benayad, E. Dunina, A. Kornienko, L. Fomicheva, A. Braud, and P. Camy, "Emission properties of Tm^{3+}-doped CaF₂, KY₃F₁₀, LiYF₄, LiLuF₄ and BaY₂F₈ crystals at 1.5 µm and 2.3 µm," J. Lumin. **225**, 117279 (2020).

23. B. M. Walsh, N. P. Barnes, M. Petros, J. Yu, and U. N. Singh, "Spectroscopy and modeling of solid state lanthanide lasers: Application to trivalent Tm^{3+} and Ho^{3+} in YLiF4 and LuLiF4," J. Appl. Phys. **95**(7), 3255–3271 (2004).

24. E. Y. Perlin, A. M. Tkachuk, M.-F. Joubert, and R. Moncorge, "Cascade-avalanche up-conversion in Tm^{3+}:YLF crystals," Opt. Spectrosc. **90**(5), 691–700 (2001).

25. L. Guillemot, "Etude de la transition 3H4→3H5 de l'ion Tm^{3+} pour une émission laser moyen infrarouge (entre 2 et 3µm)," PhD thesis, University of Caen Normandy (2021).

26. P. F. Moulton, G. A. Rines, E. V. Slobodtchikov, K. F. Wall, G. Frith, B. Samson, and A. L. G. Carter, "Tm-doped fiber lasers: Fundamentals and power scaling," IEEE J. Sel. Top. Quantum Electron. **15**(1), 85–92 (2009).

27. M. Tao, Q. Huang, T. Yu, P. Yang, W. Chen, and X. Ye, *Cross relaxation in Tm-doped fiber lasers*, S. Kaierle, J. Liu, and J. Cao, eds. (2013), p. 87961W. 10.1117/12.2011078

28. J. I. Mackenzie, S. So, D. P. Shepherd, and W. A. Clarkson, "Comparison of laser performance for diode-pumped Tm:YLF of various doping concentrations," in *Advanced Solid-State Photonics (TOPS)* (OSA, 2005), p. 202.

29. A. Berrou, D. Morris, O. J. Collett, and M. J. D. Esser, "Comparative study of high power Tm:YLF and Tm:LLF slab lasers," in *High-Brightness Sources and Light-Driven Interactions* (OSA, 2018), p. MM2C.4.

30. X. Yu, Z. Pan, H. Chu, F. Zha, H. Pan, L. Ma, P. Loiko, P. Camy, and D. Li, "Cascade lasing at ~2 μm and ~2.3 μm in a diode-pumped Tm:YVO$_4$ laser," Opt. Express **31**(9), 13576 (2023).

31. X. Yu, H. Chu, F. Zha, H. Pan, S. Zhao, Z. Pan, and D. Li, "Watt-level diode-pumped Tm:YVO$_4$ laser at 2.3 μm," Opt. Lett. **47**(21), 5501 (2022).

32. X. Yu, Z. Pan, H. Chu, H. Pan, S. Zhao, and D. Li, "Diode-pumped efficient high-power cascade Tm:GdVO$_4$ laser simultaneously operating at ~2 μm and ~2.3 μm," Opt. Express **31**(16), 26368 (2023).